



---

## Investigation of Adsorptive Properties of Modified Sepiolite as an Efficient Magnetically Recoverable Clay for Removal of Azo Dye from Aqueous Solutions

Nahid Rasouli\*, Somayea Batavani

Department of Chemistry, Payame Noor University, P.O. Box 19395-3697, Tehran, Iran

**Abstract** In this research, the natural clay of sepiolite ( $Mg_4Si_6O_{15}(OH)_2 \cdot 6H_2O$ ) were modified by magnetic metal oxide of  $Ni_{0.5}Zn_{0.5}Fe_2O_4$  to obtain an efficient and magnetically recoverable adsorbent ( $Ni_{0.5}Zn_{0.5}Fe_2O_4$ /sepiolite). The synthesized adsorbent ( $Ni_{0.5}Zn_{0.5}Fe_2O_4$ /sepiolite) was characterized by X-ray diffraction (XRD), Fourier transform infrared (FT-IR), UV-Vis spectroscopy, scanning electron microscopy (SEM) and energy dispersive X-ray analysis (EDX). In this study, the adsorption properties of the prepared sample was evaluated for the removal of Congo red (CR) dye in aqueous solution and the reusability of the sample was also investigated. The effect of initial dye concentration, pH and temperature on adsorption capacity of modified clay ( $Ni_{0.5}Zn_{0.5}Fe_2O_4$ /sepiolite) for Congo red were investigated. Also, the results of adsorption kinetic of CR dye in aqueous solution followed pseudo- first order model.

**Keywords** Azo dye; adsorption kinetic; sepiolite; Magnetic; recoverable clay

---

### Introduction

Dyes are widely used in industries such as textiles, leather, printing, food, and plastics, etc. The removal of dyes from industrial wastewaters is a major problem [1-2]. Conventional methods for the removal of dyes from wastewater include adsorption onto solid substrates, chemical coagulation, oxidation, filtration and biological treatment. Adsorption is one of the effective separation techniques to remove dilute pollutants [3-4]. Therefore, researches have been continued a search for cheaper, easily obtainable materials for the adsorption of dye. Natural clays for dye removal from wastewater such as sepiolite are investigated as low-cost and readily available adsorbents. The adsorption capacity of clays results from high surface area and a net negative charge on their structure, which attracts and holds cations such as heavy metals [5]. Sepiolite is a natural hydrated magnesium silicate with a wide range of industrial applications derived mainly from its adsorptive properties. It has a fibrous structure formed by an alteration of blocks and channels that grow up in the fiber direction. Each block is constructed of two tetrahedral silica sheets enclosing a central magnesia sheet. Adsorption is due to the presence of active adsorption centers on sepiolite surfaces (oxygen atoms in the tetrahedral sheet, water molecules coordinated with the  $Mg^{2+}$  ions at the edge of the structure, and silanol groups caused by the break-up of Si—O—Si bonds) [6-7]. The ability of sepiolite for adsorption of cationic dyes has been reported [8–11]. Regarding anionic dyes, natural sepiolite provided relatively low adsorbed amounts of an azo acid dye [12]. In its untreated form, sepiolite was not also able to remove anionic dyes, requiring a chemical modification [13]. Recently, studies on magnetic nanoparticles has grown intensely. It is believed that magnetic nanoparticles can be used as modifier which exhibit high adsorption, chemical and thermal stability. In addition, the easy separation of magnetic adsorbent from solution can be achieved using an external magnetic field [14–16]. So, the aim of this work is to examine the effectiveness of



sepiolite modified by magnetic metal oxide ( $\text{Ni}_{0.5}\text{Zn}_{0.5}\text{Fe}_2\text{O}_4/\text{sepiolite}$ ) as low cost material in removing high concentration of Congo red from aqueous solution. Also, the adsorption rates were determined quantitatively and simulated with the pseudo-first order and pseudo second order kinetic models.

## 2. Experimental

### 2.1. Materials and characterization

All the analytical chemicals ( $\text{Fe}(\text{NO}_3)_3 \cdot 9\text{H}_2\text{O}$ ,  $\text{Ni}(\text{NO}_3)_2 \cdot 6\text{H}_2\text{O}$ ,  $\text{Zn}(\text{NO}_3)_2 \cdot 6\text{H}_2\text{O}$ , sodium hydroxide and Congo red dye were purchased from Merck and used without further purification. The sepiolite clay used in this study was provided from Neishabour Region, Iran. Congo red dye used in this study was obtained from Sigma. The molecular structure of this dye is shown in Fig.1. The structural analysis of the samples was performed by powder X-ray Diffraction (Holland Philips Expert, X-ray diffractometer with Cu-K $\alpha$  radiation) and FT-IR analysis using a Fourier transmission infrared spectrometer (JASCO FTIR-4200, Japan) in KBr pellet, in the range of 4000-400  $\text{cm}^{-1}$ . The morphology of the samples was characterized by scanning electron microscopy, SEM (VEGA3, TESCAN). The UV-Vis absorption spectra were recorded using a Shimadzu UV-2550 spectrophotometer.

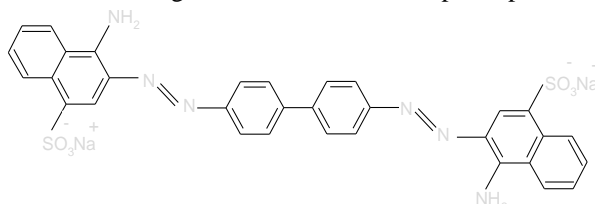


Figure 1: The chemical structure of CR dye

### 2.2. Synthesis of the modified Sepiolite ( $\text{Ni}_{0.5}\text{Zn}_{0.5}\text{Fe}_2\text{O}_4/\text{sepiolite}$ )

The modified sepiolite was prepared by co-precipitation method. In this method, 3 g sepiolite was added into 100 ml of distilled water containing  $\text{Ni}(\text{NO}_3)_2 \cdot 6\text{H}_2\text{O}$  (0.02 mol),  $\text{Zn}(\text{NO}_3)_2 \cdot 6\text{H}_2\text{O}$  (0.02 mol) and  $\text{Fe}(\text{NO}_3)_3 \cdot 9\text{H}_2\text{O}$  (0.04 mol). Then, the pH of solution was adjusted to 10 by adding  $\text{NH}_4\text{OH}$  solution (4 mol  $\text{L}^{-1}$ ). The suspension was left to settle down and filtrated. Finally, the obtained solid was washed with distilled water three times and dried at 80°C for 12 h.

### 2.3. Adsorption experiments

In order to investigate the behavior of the natural sepiolite and  $\text{Ni}_{0.5}\text{Zn}_{0.5}\text{Fe}_2\text{O}_4/\text{sepiolite}$ , dark adsorption experiments were carried out. The amount of adsorbed dye per gram of adsorbent (mg/g) at time t (min) was calculated using the following equation [17]:

$$q_t = \frac{(C_0 - C_t)V}{m} \quad (1)$$

Where  $q_t$  ( $\text{mgg}^{-1}$ ) is the amount of adsorbed Congo red per gram of adsorbent at time t (min),  $C_0$  is the initial concentration of Congo red solution ( $\text{mgL}^{-1}$ ),  $C_t$  is the concentration of Congo red solution ( $\text{mgL}^{-1}$ ) at time t (min), V is the volume of the solution (L) and m is the mass of the adsorbent (g). The initial concentrations of dye solutions were in the range of 40 to 100 mg/L and experiments were performed at 25 °C. The initial dye concentration, pH, and temperature were selected as experimental parameters. The effects of pH on the dye adsorption were determined over a range of pH 7-13. The pH of the solution was adjusted with NaOH or  $\text{HNO}_3$  solution by using a pH-meter. After the adsorption equilibrium is reached, the suspensions were centrifuged at 15000 rpm and the concentration of dye remaining in the supernatant determined using UV-vis spectrophotometer at  $\lambda_{\text{max}} = 498$  nm. The amount of adsorbed dye was calculated from the concentrations in the solution both before and after the adsorption. The calibration curve was plotted from the dye solutions prepared in the concentrations of 40–100 mg/L. All experiments were repeated at least twice.

### 2.4. Kinetic studies

The Adsorption kinetics was determined by analyzing the adsorptive uptake of dye from aqueous solution at several times intervals. In this work, 100 cc of aqueous solution of CR dye with an initial concentration of 80mg/L were poured in glass tube and mixed with 0.05g of adsorbent at room temperature. Then, at time intervals between 15 to 180 min, the solid phase was separated by centrifugation at 1500 rpm. The dye concentration in the supernatant

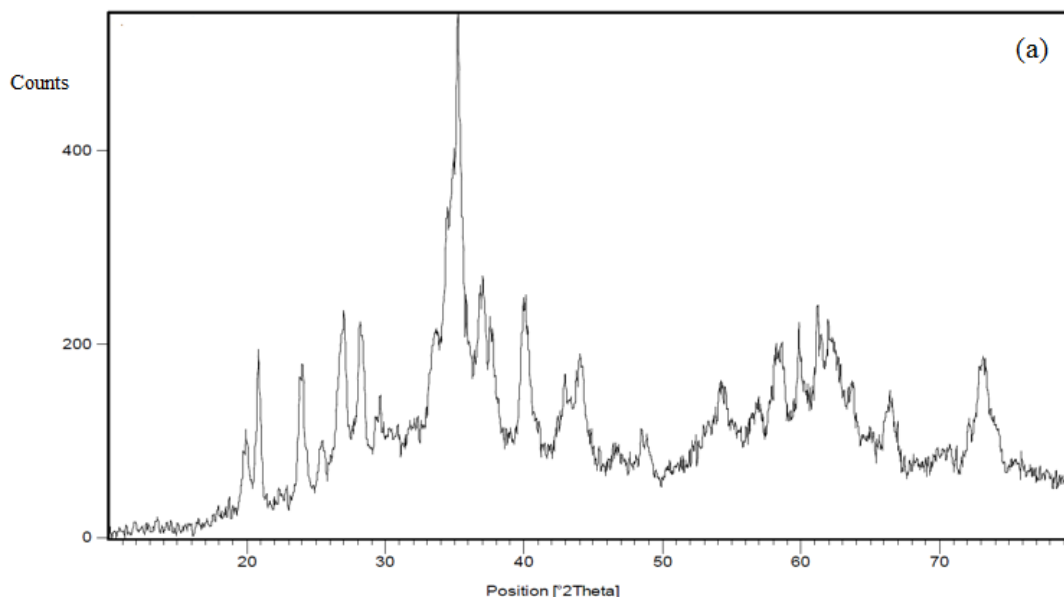


liquid was determined by UV-vis spectrophotometer. The measurements were carried out at the wavelength  $\lambda_{\max}=498$  nm for CR dye.

### 3. Results and Discussion

#### 3.1. Characterization of the modified sepiolite ( $Ni_{0.5}Zn_{0.5}Fe_2O_4$ /sepiolite)

Fig. 2 (a-c) shows the XRD patterns of  $Ni_{0.5}Zn_{0.5}Fe_2O_4$ /sepiolite,  $Ni_{0.5}Zn_{0.5}Fe_2O_4$  and sepiolite, respectively. The XRD pattern of  $Ni_{0.5}Zn_{0.5}Fe_2O_4$ /sepiolite show that the  $Ni_{0.5}Zn_{0.5}Fe_2O_4$  with cubic phase was obtained (JCPDS No.08-0234), and the distinctive peaks at  $29.92^\circ$ ,  $35.27^\circ$ ,  $42.85^\circ$ ,  $53.11^\circ$ ,  $56.63^\circ$  and  $62.21^\circ$  matched well with the (220), (311), (400), (422), (511) and (440) crystal planes of  $Ni_{0.5}Zn_{0.5}Fe_2O_4$  [18]. Other crystal phases corresponding to peaks at 7.18, 19.70, 20.58, 23.74, 26.65, 27.98, 34.74, 36.81 and  $39.86^\circ$  were compared with the  $2\theta$  values reported for sepiolite [19]. However, it could be noticed that the characteristic diffraction peak of sepiolite in the  $Ni_{0.5}Zn_{0.5}Fe_2O_4$ /sepiolite composite was weak, which could be attributed to the low amount of the sepiolite is used in the synthesis of composite. The chemical structure of the  $Ni_{0.5}Zn_{0.5}Fe_2O_4$ /sepiolite composite was confirmed by FT-IR analysis. The FT-IR spectrum of sepiolite has the characteristic bands at  $3691\text{ cm}^{-1}$  related to stretching vibrations of hydroxyl groups attached to octahedral Mg ions located in the interior blocks,  $3581\text{ cm}^{-1}$  related to H–O–H stretching vibrations of water molecules weakly hydrogen bonded to the Si–O surface, and  $3452\text{ cm}^{-1}$  and  $1663\text{ cm}^{-1}$  related to the water –OH stretch and bending vibration, respectively. In addition, the spectrum of natural sepiolite had also the characteristic lattice vibrations at  $1211$ ,  $1090$  and  $984\text{ cm}^{-1}$  (the Si–O combination bands),  $1017\text{ cm}^{-1}$  (the basal plane of the tetrahedral units exhibiting the Si–O–Si plane vibrations),  $450\text{ cm}^{-1}$  (Si–O–Mg of the octahedral–tetrahedral linkage) and  $650\text{ cm}^{-1}$  ( $Mg_3OH$ -bending vibration) [19-21]. The morphology of sepiolite can be seen in the SEM images (Fig.3(a)). SEM image of the sepiolite showed that it has a fibrous structure that there is possibility for dye to trapped and adsorbed into this structure. However, SEM image of the  $Ni_{0.5}Zn_{0.5}Fe_2O_4$ /sepiolite sample is different from sepiolite sample (Fig.3(b)). The EDX spectrum of  $Ni_{0.5}Zn_{0.5}Fe_2O_4$ /sepiolite is shown in Fig. 4(b). The atomic weight ratio of O: Mg: Si: Fe: Ni: Zn was 66.74: 8.52: 12.95: 5.07: 0.99: 0.92 which indicates that the natural sepiolite are successfully modified by  $Ni_{0.5}Zn_{0.5}Fe_2O_4$  sample. Based on the results of XRD, FT-IR, SEM and EDAX confirmed the synthesis of the  $Ni_{0.5}Zn_{0.5}Fe_2O_4$ /sepiolite composite.



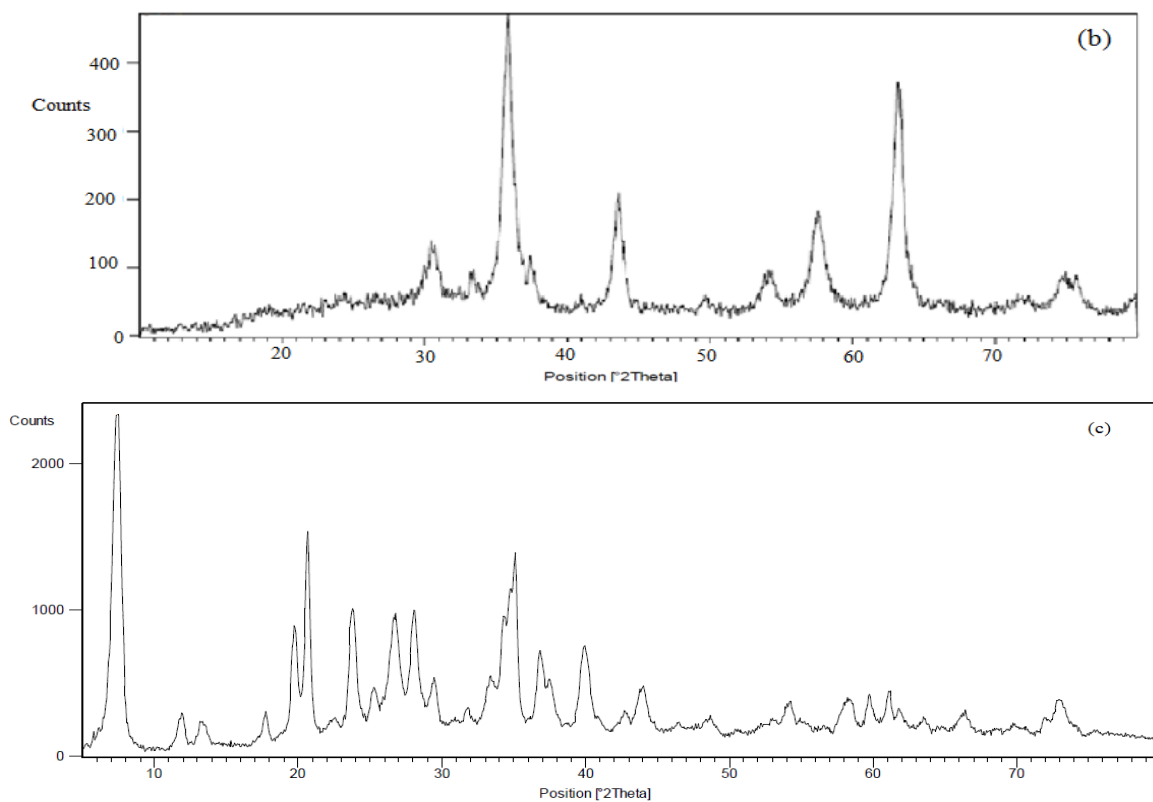


Figure 2: The XRD patterns of (a)  $Ni_{0.5}Zn_{0.5}Fe_2O_4$ /sepiolite, (b)  $Ni_{0.5}Zn_{0.5}Fe_2O_4$  and (c) sepiolite samples

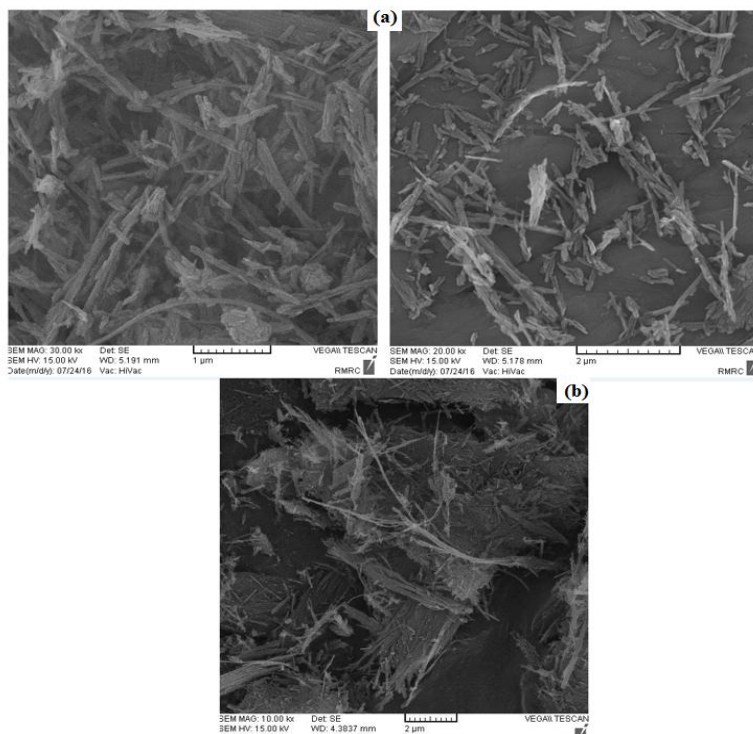


Figure 3: SEM images of the (a) sepiolite and (b)  $Ni_{0.5}Zn_{0.5}Fe_2O_4$ /sepiolite samples

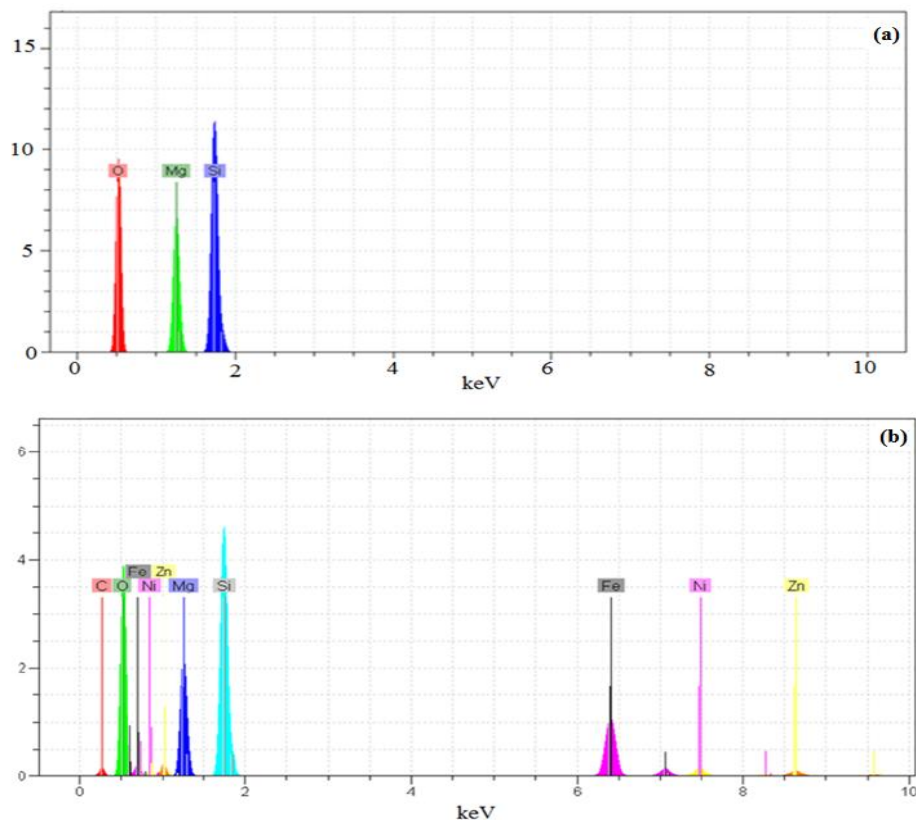


Figure 4: EDAX spectrum of (a) sepiolite and (b) Ni<sub>0.5</sub>Zn<sub>0.5</sub>Fe<sub>2</sub>O<sub>4</sub>/sepiolite samples

### 3.2. Adsorption properties

The adsorption kinetic experiments were carried out at different experimental conditions and the results obtained are discussed below.

#### 3.2.1. Effect of dye concentration

The initial concentration provides an important driving force to overcome all mass transfer resistances of all molecules between the aqueous and solid phases. Fig. 5 shows the plot of amount of dye adsorbed versus time at different initial dye concentrations. From the figure it was observed that the amount of dye adsorbed gets increased. Dye removal is highly concentration dependent. The rate of adsorption also increases with the increase in initial dye concentration due to increase in the driving force. In fact, the more concentrated the solution, the better the adsorption.

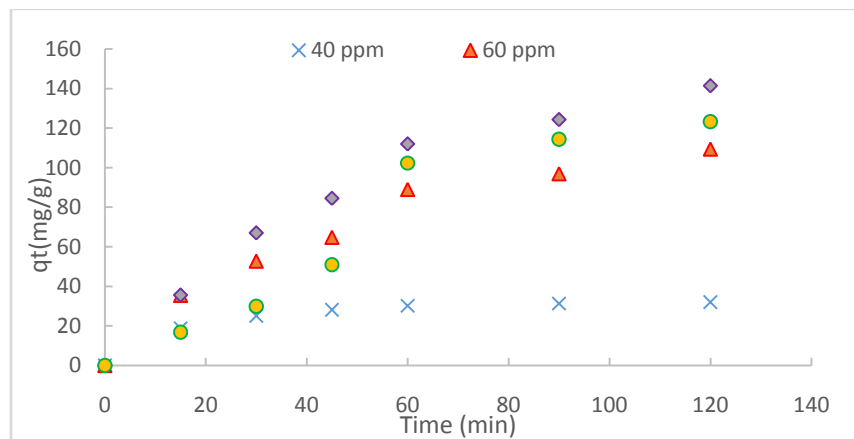


Figure 5: The effect of initial dye concentration on the adsorption rate of CR dye on  $Ni_{0.5}Zn_{0.5}Fe_2O_4$ /sepiolite

### 3.2.2. Effect of solution pH

Generally, the adsorption capacity increases with increasing pH for cationic dyes, while it decreases with increasing pH for anionic dyes. We had previously shown that sepiolite had an isoelectrical point at pH 6.6 and exhibited positive zeta potential values at the lower pH values from pH 6.6, and negative zeta potential values at the higher pH values from pH 6.6. Fig. 6 demonstrates that the adsorption decreases with increasing pH because of the electrostatic repulsion between the chromophore groups of dye and the negatively charged sepiolite surface. The higher adsorption of CR dye on sepiolite at neutral pH result due to the neutralization of the negative sites at the surface of sepiolite.

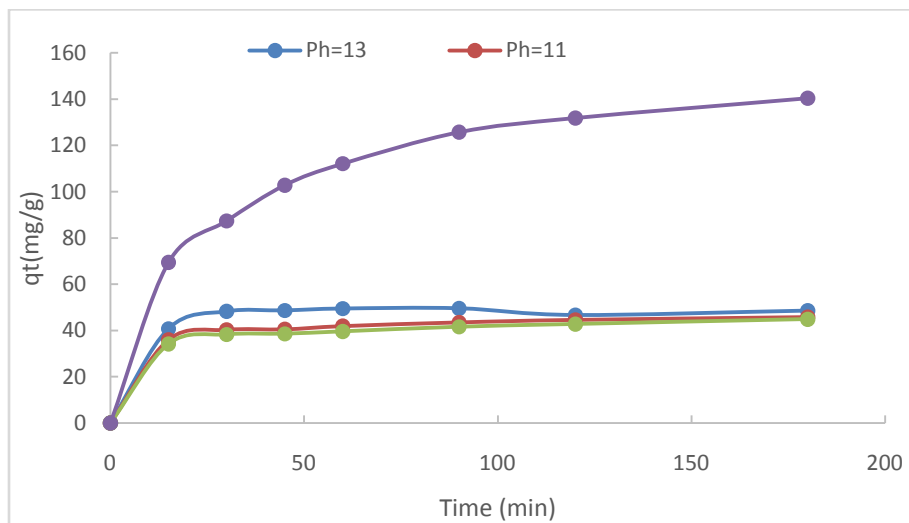


Figure 6: The effect of pH on the adsorption rate of CR dye on  $Ni_{0.5}Zn_{0.5}Fe_2O_4$ /sepiolite.

### 3.2.3. Effect of temperature

The temperature has two major effects on the adsorption process. Increasing the temperature is known to increase the rate of diffusion of the adsorbate molecules across the external boundary layer and in the internal pores of the adsorbent, owing to the decrease in the viscosity of the solution. In addition, changing the temperature will change the equilibrium capacity of the adsorbent for a particular adsorbate. As seen in Fig. 7, the adsorbed amount of CR at equilibrium has increased with increase in temperature. This may be a result of increase in the mobility of the large dye ion with temperature. An increasing number of molecules may also acquire sufficient energy to undergo an interaction with active sites at the surface. Therefore, it can be said that the adsorption process is endothermic

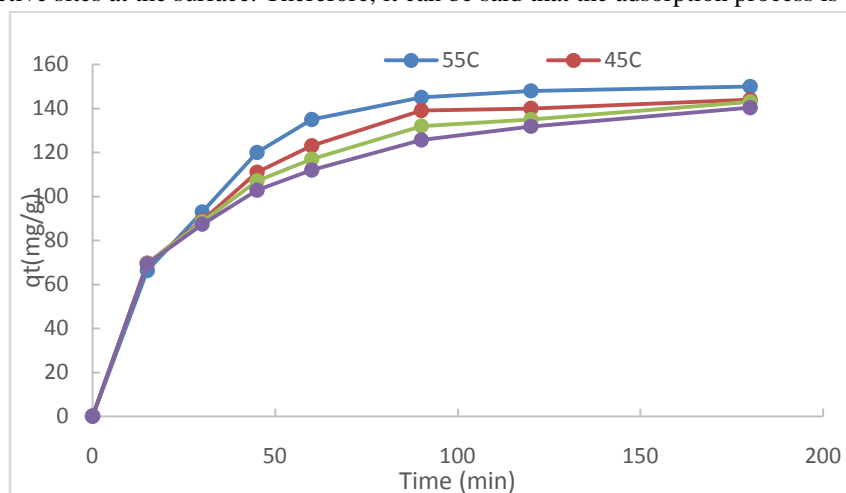


Figure 7: The effect of temperature on the adsorption rate of CR dye on  $Ni_{0.5}Zn_{0.5}Fe_2O_4$ /sepiolite



### 3.3.4. Adsorption kinetic models

The kinetic of adsorption can be described using several models. In the present study, the Lagergren pseudo- first- and pseudo- second order model was tested. The Lagergren's pseudo- first order model for liquid-solid adsorption is generally expressed as: [23, 24]

$$\frac{dq_t}{dt} = k_1(q_e - q_t) \quad (2)$$

Here  $k_1$  is rate constant for pseudo- first order adsorption. After definite integration by applying the initial conditions  $q_t=0$  at  $t=0$  and  $q_t=q_t$  at  $t=t$ , Eq. (2) becomes:

$$\ln(q_e - q_t) = \ln(q_e) - k_1 t \quad (3)$$

The above linear equation can usually be used to estimate equilibrium adsorption capacity ( $q_e$ ) from intercept and  $k_1$  from the slope. A pseudo- second order equation can be expressed as follows [25, 26]:

$$\frac{dq_t}{dt} = k_2(q_e - q_t)^2 \quad (4)$$

Where  $k_2$  is rate constant for pseudo- second order adsorption. After definite integration by applying the initial conditions, we have a linear form as:

$$\frac{t}{q_t} = \frac{1}{k_2 q_e^2} + \frac{1}{q_e} t \quad (5)$$

The plot of  $t/q_t$  versus time gives straight lines. The values for  $q_e$  and  $k_2$  can be calculated from the slope and intercept. The pseudo- second order equation is often successfully used to describe the kinetics of pollutants on the adsorbent. This model assumes that chemisorption might be the rate limiting step in adsorption processes [27, 28]. Fig. 8 (a) & (b) represents a pseudo- first and pseudo- second order kinetic model for adsorption of CR at 25 °C for the  $\text{Ni}_{0.5}\text{Zn}_{0.5}\text{Fe}_2\text{O}_4$ /sepiolite sample. The correlation coefficient ( $R^2$ ) for the pseudo- second order model did not fit very well for the  $\text{Ni}_{0.5}\text{Zn}_{0.5}\text{Fe}_2\text{O}_4$ /sepiolite sample and calculated  $q_e$  value was near to the experimental data. For pseudo- first order kinetic, the  $R^2$  is closer to unity. These results show that the pseudo- first order model is predominant. This model assumes that chemisorption might be the rate limiting step in adsorption processes. The stability of the samples was investigated during four cycles of experiment for adsorption of CR dye. This properties is very important in the application of the  $\text{Ni}_{0.5}\text{Zn}_{0.5}\text{Fe}_2\text{O}_4$ /sepiolite sample in environmental technology. The reusability of the  $\text{Ni}_{0.5}\text{Zn}_{0.5}\text{Fe}_2\text{O}_4$ /sepiolite sample after several consecutive uses was obtained to be 98, 93, 90, 85 %, respectively (Fig.9).

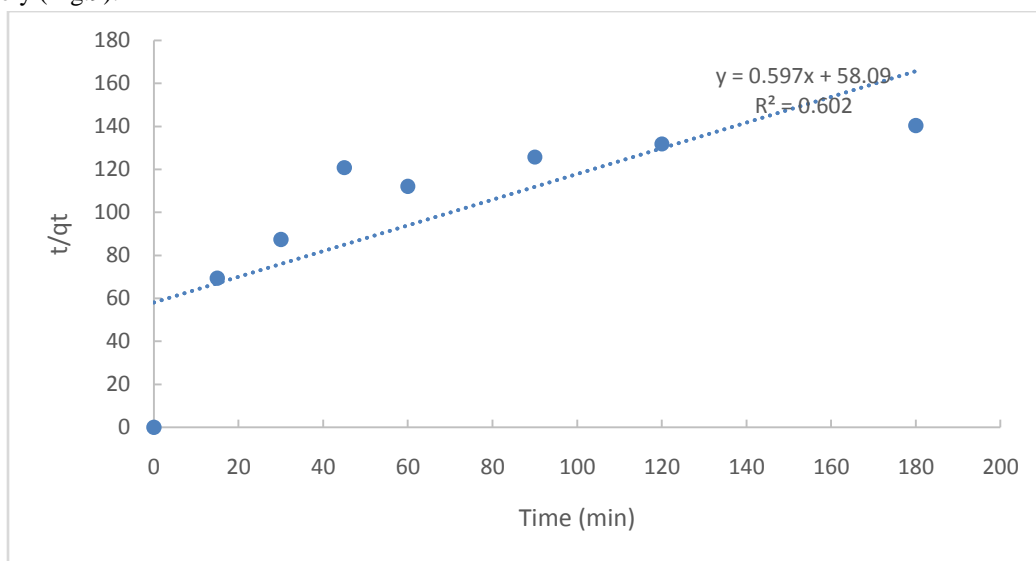


Fig.8 (a)



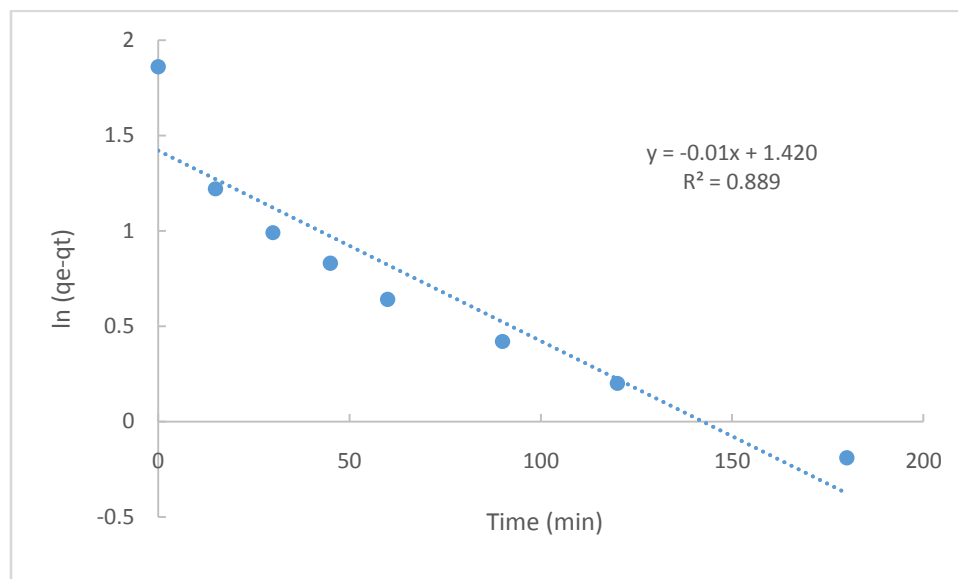


Fig.8 (b)

Figure 8(a): The plots of  $\ln(q_e - q_t)$  and (b)  $t/q_t$  versus time for  $Ni_{0.5}Zn_{0.5}Fe_2O_4$ /sepiolite samples



Figure 9: The reusability  $Ni_{0.5}Zn_{0.5}Fe_2O_4$ /sepiolite samples after four consecutive uses

#### 4. Conclusion

In our study,  $Ni_{0.5}Zn_{0.5}Fe_2O_4$  /sepiolite as an adsorbent has a high potential for removing of Congo red from the aqueous solution. The kinetics of Congo red adsorption was examined by using the pseudo-first order and pseudo-second order kinetic models under different conditions. The results of adsorption kinetic of CR dye in aqueous solution followed pseudo- first order model.

#### Acknowledgments

We are grateful to the Research Council of Payame Noor University for their financial supports.



## References

1. Chung, K.T., & Cerniglia, C.E. (1992). Mutagenicity of azo dyes—structure–activity- relationships. *Mutation Research*, 277: 201–220.
2. Garg, A., Bhat, K.L., & Bock, C.W. (2002). Mutagenicity of aminoazobenzene dyes and related structures: a QSAR/QPAR investigation. *Dyes and Pigments*, 55: 35–52.
3. Ayoub, G.M., Hamzeh, A., & Semerjian, L. (2011). Post treatment of tannery wastewater using lime/bittern coagulation and activated carbon adsorption. *Desalination*, 273: 359–365.
4. Papadia, S., Rovero, G., Fava, F., & Di Gioia, D. (2011). Comparison of different pilot scale bioreactors for the treatment of a real wastewater from the textile industry. *International Biodeterioration and Biodegradation*, 65: 396–403.
5. Khenifi, A. (2007). Adsorption study of an industrial dye by an organic clay. *Adsorption*, 13(2): 149–158.
6. Ruiz-Hitzky, E. (2001). Molecular access to intracrystalline tunnels of sepiolite. *Journal of Materials Chemistry*, 11: 86–91.
7. Yariv, S. (1996). Thermo-IR-spectroscopy analysis of the interactions between organic pollutants and clay minerals. *Thermochimica Acta*, 274:1–35.
8. Han, Z.X., Zhu, Z., Wu, D.D., Wu, J., & Liu, Y.R. (2014). Adsorption kinetics and thermodynamics of acid blue 25 and methylene blue dye solutions on natural sepiolite. *Synthesis and Reactivity in Inorganic and Metal-Organic Chemistry*, 44: 140–147.
9. Lazarevic, S., Jankovic-Castvan, I., Jovanovic, D., Milonjic, S., Janackovic, D., & Petrovic, R. (2007). Adsorption of  $Pb^{2+}$ ,  $Cd^{2+}$  and  $Sr^{2+}$  ions onto natural and acid-activated sepiolites. *Applied Clay Science*, 37: 47–57.
10. Rytwo, G., Nir, S., Margulies, L., Casal, B., Merino, J., Ruiz-Hitzky, E., & Serratos, J.M. (1998). Adsorption of monovalent organic cations on sepiolite: experimental results and model calculations. *Clays and Clay Minerals*, 46: 340–348.
11. Santos, S.C.R., & Boaventura, R.A.R. (2008). Adsorption modelling of textile dyes by sepiolite. *Applied Clay Science*, 42: 137–145.
12. Tumsek, F., & Avci, O. (2013). Investigation of kinetics and isotherm models for the acid orange 95 adsorption from aqueous solution onto natural minerals. *Journal of Chemical & Engineering Data*, 58: 551–559.
13. Ozdemir, O., Armagan, B., Turan, M., & Celik, M.S. (2004). Comparison of the adsorption characteristics of azo-reactive dyes on mesoporous minerals. *Dyes and Pigments*, 62: 49–60.
14. Banerjee, S., Sharma, G.C., Chattopadhyaya, M.C., & Sharma, Y.C. (2014). Kinetic and equilibrium modeling for the adsorptive removal of methylene blue from aqueous solutions on of activated fly ash (AFSH). *Journal of Environmental Chemical Engineering*, 2: 1870–1880.
15. Cardoso, N.F., Lima, E.C., Pinto, I.S., Amavisca, C.V., Royer, B., Pinto, R.B., Alencar, W.S., & Pereira, S.F.P. (2011). Application of cupuassu shell as biosorbent for the removal of textile dyes from aqueous solution. *Journal of Environmental Management*, 92: 1237–1247.
16. Pavan, F.A., Camacho, E.S., Lima, E.C., Dotto, G.L., Branco, V.T.A., & Dias, S.L.P. (2014). Formosa papaya seed powder (FPSP): Preparation, characterization and application as an alternative adsorbent for the removal of crystal violet from aqueous phase. *Journal of Environmental Chemical Engineering*, 2:230–238.
17. Belessi, V., Romanos, G., Boukos, N., Lambropoulou, D., & Trapalis, C. (2009). Removal of Reactive Red 195 from aqueous solutions by adsorption on the surface of  $TiO_2$  nanoparticles. *Journal of Hazardous Materials*, 170: 836–844.
18. Kasi Viswanath, I. V., Murthy, Y. L. N., Raotat, K., & Singh, R. (2015). Synthesis and characterization of nano ferrites by citrate gel method. *International Journal of Chemical Sciences*, 11(1): 64–72.



19. Brindley, G.W. (1959). X-ray and electron diffraction data for sepiolite. *American Mineralogist*, 44: 495-500.
20. Eren, E., Cubuk, O., Ciftci, H., Eren, B., & Caglar, B. (2010). Adsorption of basic dye from aqueous solutions by modified sepiolite: equilibrium, kinetics and thermodynamics study. *Desalination*, 252: 88-96.
21. Ozcan, A., & Ozcan, A.S. (2005). Adsorption of Acid Red 57 from aqueous solutions onto surfactant-modified sepiolite. *Journal of Hazardous Materials*, B125: 252-259.
22. Belessi, V., Romanos, G., Boukos, N., Lambropoulou, D., & Trapalis, C. (2009). Removal of Reactive Red 195 from aqueous solutions by adsorption on the surface of TiO<sub>2</sub> nanoparticles. *Journal of Hazardous Materials*, 170: 836-844.
23. Khan, Y., Durrani, S.K., Siddique, M., & Mehmood, M. (2011). Hydrothermal synthesis of alpha Fe<sub>2</sub>O<sub>3</sub> nanoparticles capped by Tween-80. *Materials Letters*, 65: 2224-2227.
24. Eftekhari, S., Habibi-Yangjeh, A., & Sohrabnezhad, S. (2010). Application of AlMCM-41 for competitive adsorption of methylene blue and rhodamine B: Thermodynamic and kinetic studies. *Journal of Hazardous Materials*, 178: 349-355.
25. Ho, Y.S. (2006). Review of second-order models for adsorption systems. *Journal of Hazardous Materials*, 136: 681-689.
26. Yuh-Shan, H. (2004). Citation review of Lagergren kinetic rate equation on adsorption reactions. *Scientometrics*, 59: 171-177.
27. Inyinbor, A.A., Adekola, F.A., & Olatunji, G.A. (2016). Kinetics, isotherms and thermodynamic modeling of liquid phase adsorption of Rhodamine B dye onto *Raphia hookerie* fruit epicarp. *Water Resources and Industry*, 15: 14-27.
28. Muthukumar, C., Sivakumar, V. M., & Thirumarimurugan, M. (2016). Adsorption isotherms and kinetic studies of crystal violet dye removal from aqueous solution using surfactant modified magnetic nanoadsorbent. *Journal of the Taiwan Institute of Chemical Engineers*, 63: 354-362.

